Evaluation of Transparent Carbon Nanotube Networks of Homogeneous Electronic Type

Roderick K. Jackson,[†] Andrea Munro,[‡] Kenneth Nebesny,[‡] Neal Armstrong,[‡] and Samuel Graham[†,*]

[†]School of Mechanical Engineering, Georgia Institute of Technology, Atlanta, Georgia 30332 and [‡]Department of Chemistry and College of Optical Sciences, University of Arizona, Tucson, Arizona 85721

ABSTRACT In this report, we present a description of the optical and electronic properties of as-deposited, annealed, and chemically treated single-walled carbon nanotube (SWNT) films showing metallic or semiconducting behavior. As-deposited and annealed semiconducting SWNT films were significantly less conductive than metallic SWNT films; however, chemical treatment of semiconducting SWNT films resulted in sheet resistance values as low as 60 $\Omega \cdot sq^{-1}$ in comparison to 76 $\Omega \cdot sq^{-1}$ for similarly processed metallic SWNT films. We conclude that the greater improvement of electrical conductivity observed in the semiconducting SWNT film results from the difference in the density of available electronic states between metallic and semiconducting SWNTs. A corroborative investigation of the change in surface work function and the chemical composition of SWNT films, as revealed by X-ray photoelectron spectroscopy, is provided to support these conclusions and to give new perspective to the formation of electronically homogeneous SWNT networks.

KEYWORDS: transparent electrodes · carbon nanotubes · Fermi level · doping · work function

Single-walled carbon nanotube (SWNT) semitransparent thin film networks are being developed to provide an alternative to transparent conducting oxides (TCO) in electronic devices, such as organic photovoltaics (OPV) and organic light-emitting diodes (OLEDs).[1,2] Previously developed SWNT networks have generally consisted of a heterogeneous mixture of nanotubes with metallic and semiconducting behavior with ratios of metallic/semiconducting tubes being *ca.* 1:2. Heterogeneous mixtures yield transparent electrodes with optoelectronic properties comparable to indium tin oxide (ITO) deposited on plastic substrates.[3] However, the sheet resistance and transmittance of these SWNT films have yet to compete favorably with TCOs on glass substrates.[4] The ease of low-temperature processing SWNTs as thin films and their potentially improved compatibility with other electronically active organic thin film materials motivate research to further improve their thin film optical and electronic properties. In order to fully realize the potential of SWNT networks in organic electronic devices, it will be necessary to utilize monodisperse networks that leverage the electronic homogeneity of the film to achieve optimal device performance. Progress in the efficient separation of SWNTs by electronic type now allows for such an approach to be taken.[5,6]

SWNTs can be classified as either metallic or semiconducting in behavior based on the chirality of the tube.[7] However, because SWNTs are 1-D in structure, the traditional metal/semiconductor classifications are no longer strictly valid. In particular, metallic SWNTs have a relatively small density of states (DOS) at the Fermi energy when compared to traditional bulk metals.[8] On the other hand, semiconducting SWNTs can have a larger density of electronic states within the valence band, in comparison to metallic SWNTs at a similar energy level.[9] A full understanding of the effect of this departure from a traditional classification of metals and semiconductors has yet to be achieved.

It has been shown that heterogeneous films of metallic and semiconducting SWNTs can be effectively p-doped *via* chemical treatment with HNO_3 and $SOCl_2$ for improved conductivity.[10,11] The optoelectronic impact of doping, however, differs significantly between metallic and semiconducting SWNT films as recently reported by Blackburn *et al.*[12] In their study, films of monodisperse doped metallic SWNTs were higher in electrical resistance than similarly processed homogeneous networks of degenerately doped semiconducting SWNTs. This result is contrary to a conventional understanding of metals and semiconductors but is consistent with a more fundamental appreciation of conduction through nanotube networks, as will be

*Address correspondence to sgraham@gatech.edu.

Received for review August 13, 2009 and accepted February 02, 2010.

Published online March 4, 2010.
10.1021/nn9010076

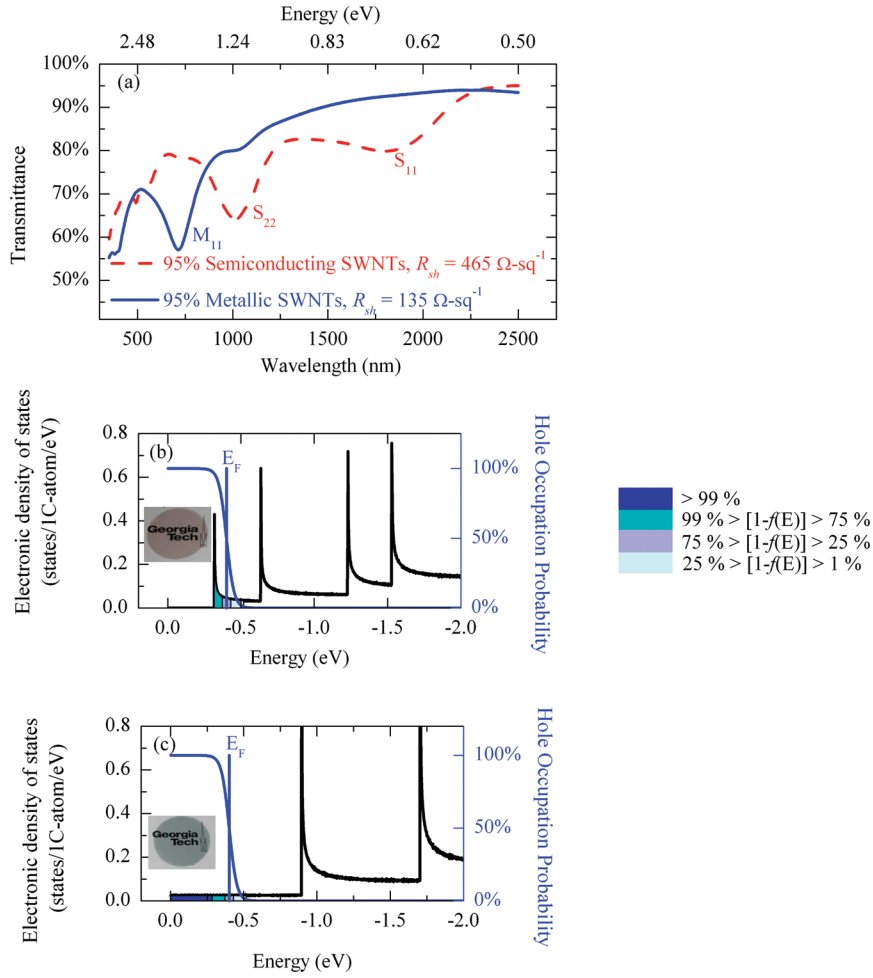

Figure 1. (a) Optical transmittance spectra of as-deposited metallic and semiconducting SWNT films. Energy transitions at S_{11}, S_{22}, and M_{11} van Hove singularities are labeled. (b) (11,10) Semiconducting SWNT 1-D density of states with moderate doping. Inset: Semiconducting film on glass substrate. (c) (10,10) Metallic SWNT 1-D density of states with moderate doping. Inset: Metallic film on a glass substrate.

demonstrated in this report. The goal of this work is to present a lucid description of the optoelectronic properties of as-deposited SWNT films of metallic or semiconducting behavior and elucidate the impact of doping *via* chemical treatment on each electronic type. Corroborative optical transmittance spectra, SWNT electronic band structure theory, and photoelectronic characterization are provided to support the conclusions presented.

RESULTS AND DISCUSSION

Optoelectronic Characterization of Homogeneous Metallic and Semiconductor SWNT Films. SWNT solutions with greater than 95% homogeneity by electronic type were purchased from NanoIntegris and used to prepare transparent SWNT films on glass substrates in a method similar to that described by Wu *et al.*[13] The SWNT film electrical sheet resistance, R_{sh}, was determined *via* the transmission line method described by Jackson and Graham.[14] R_{sh} of the as-deposited metallic SWNT film was less than the R_{sh} of the as-deposited semiconductor film, with values of 135 and 465 $\Omega \cdot sq^{-1}$, respectively. The optical transmittance spectra for the as-deposited metallic and semiconducting SWNT films are shown in Figure 1a. The metallic SWNT film has a transmittance at 550 nm of 70%, similar to the 72% transmittance obtained for the semiconducting film. Due to the characteristic absorption peaks of the two SWNT electronic types, clearly evident in Figure 1, a significant transmittance variation can be observed in the spectral range most important to organic electronics (*i.e.*, 400−800 nm). The average transmittances over this spectrum are 65 and 74% for the metallic and semiconducting SWNT films, respectively. The origin of the absorption peaks is illustrated in Figure 1b,c, where the electronic density of states *versus* energy from the intrinsic Fermi level, E_{Fi}, are calculated and plotted for SWNTs with (*n*,*m*) chiralities of (11,10) and (10,10).[15] The selected SWNTs have a diameter of approximately 1.4 nm and are representative of the diameter range of semiconducting and metallic SWNTs present in the SWNT networks used in this study. The (11,10) SWNT shown in Figure 1b is a semiconducting SWNT, while the (10,10) SWNT shown in Figure 1c is metallic in be-

havior. Only the band structure below E_{Fi} is shown for clarity. The optical absorption peaks observable in Figure 1a are present due to electronic transitions between mirror image van Hove singularities above and below E_{Fi}.[16] Interband energy transitions in semiconducting SWNTs are referenced as S_{11} and S_{22} for the first and second van Hove singularities, respectively, and are labeled as such in Figure 1a, while the intraband transition in metallic SWNTs is labeled as M_{11}. Of particular note is the diminished absorption of the S_{11} energy transition in contrast to the absorption expected from the semiconducting SWNT density of electronic states.

Also, plotted in Figure 1b,c are the probabilities that a particular state is filled with a hole. The room temperature hole occupation probabilities, $P(p)$, are indicated with a color gradient and are determined by

$$P(p) = 1 - f(E) \quad (1)$$

where the Fermi function, $f(E)$, describes the probability that a state at a given energy (E) is filled with an electron. Figure 1b,c illustrates a moderate doping level that results in a Fermi energy shift of approximately 0.4 eV away from E_{Fi}. A Fermi energy shift of this magnitude is estimated for the as-deposited semiconducting film in Figure 1a to account for the initial level of bleaching seen in the S_{11} absorption.

It has been shown that oxygen readily adsorbs on the surface of SWNTs, resulting in oxidation of nanotubes and consequently an increase in the hole concentration within the valence band of semiconducting SWNTs.[17,18] XPS was used to characterize the concentration and type of oxygen species within the SWNT film (see Supporting Information). The reduced optical absorption of the S_{11} energy transition is in agreement with other reports on the S_{11} sensitivity to adsorbed oxygen.[12] A moderate level of oxygen doping also accounts for the appreciable conductivity of the semiconducting SWNT film. It is expected that an intrinsic semiconducting SWNT film would be substantially more resistive than our as-deposited films, as other reports have shown.[19] In contrast, oxygen doping due to air exposure was not sufficient to induce salient changes in the absorption intensity of the M_{11} intraband transition in the metallic SWNT film.

The optical transmittance spectra for chemically treated metallic and semiconducting SWNT films are shown in Figure 2a. Similar to the as-deposited SWNT films, average transmittances of 65 and 73% over the wavelength range of 400−800 nm are observed for the metallic and semiconducting SWNT films, respectively. Postdeposition chemical treatment was achieved *via* immersion into HNO_3 followed by $SOCl_2$ (see Experimental Section). The near complete bleaching of the S_{11} and S_{22} absorption peaks is indicative of hole doping that is sufficient to shift the Fermi energy beyond the second van Hove singularity in the valence band of semiconducting SWNTs. As illustrated in Figure 2b, a

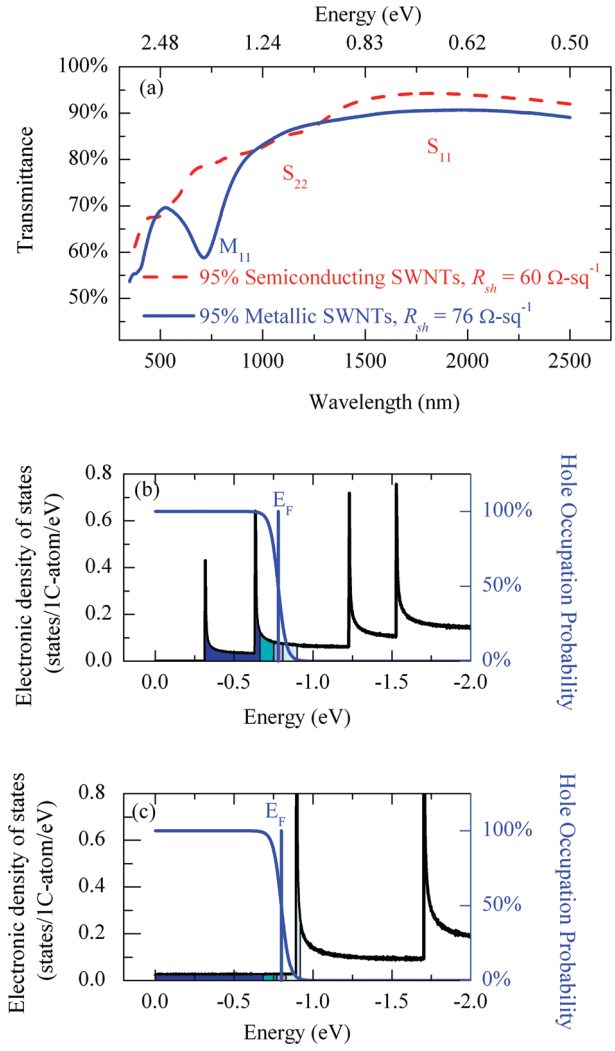

Figure 2. (a) Optical transmittance *versus* wavelength for as-deposited metallic and semiconducting SWNT films. (b) (11,10) Semiconducting SWNT 1-D density of states with substantial doping. (c) (10,10) Metallic SWNT 1-D density of states with substantial doping.

Fermi energy shift of approximately 0.8 eV from the intrinsic Fermi level would result in the occupation of holes in both van Hove singularities such that few electrons are present to transition to the mirror van Hove singularity in the conduction band. A similar absorption peak reduction at the M_{11} energy transition is not observed in Figure 2a because of the energy differences of the van Hove singularities in metallic and semiconducting SWNTs, as shown in the energy band diagrams in Figure 2b,c. The first van Hove singularity in metallic SWNTs is located approximately 0.9 eV from the E_{Fi}, compared to 0.3 and 0.6 eV for the first and second van Hove singularities in semiconducting SWNTs, respectively. The level of doping is not sufficient to shift the Fermi energy in excess of 0.9 eV from E_{Fi}, such that a significant occupation of holes in the van Hove singularity is achieved, as is illustrated in Figure 2c.

In contrast to the considerably lower conductivity of the as-deposited semiconducting SWNT film in com-

parison to the metallic SWNT film, chemical treatment resulted in comparable electrical properties between the two SWNT films. With final sheet resistance values of 60 and 76 $\Omega \cdot sq^{-1}$ for the chemically treated semiconducting and metallic SWNT films, respectively, the doped semiconducting SWNT film was observed to have a slightly higher electrical conductivity. A similar trend of a doped semiconducting film exhibiting superior conductivity to that of a doped metallic was reported by Blackburn *et al.*[12] This result can be understood by investigating the properties of individual semiconducting and metallic SWNTs. As shown in Figure 1b,c, metallic SWNTs have few electronic states at the Fermi energy, in comparison to bulk metals. This feature of metallic SWNTs allows them to be doped in such a manner as to shift the Fermi energy away from its intrinsic location. Therefore, the electronic behavior of a metallic SWNT more closely resembles the conceptual behavior of a bulk semiconductor with a nonzero density of states in the "pseudo-band gap". Also, as shown in Figures 1b,c and 2b,c, there is a larger density of electronic states within 1 eV of E_{Fi} in semiconducting SWNTs compared to metallic SWNTs at a similar energy level. The impact of the different electronic band structures of metallic and semiconducting SWNTs on electrical conduction may explain the unexpected optoelectronic observations in Figure 2a and will be discussed in the section to follow.

Electrical Conduction in SWNT Films. Electrical conduction in SWNT films can be modeled as a parallel network of 1-D conducting sticks.[20] As the resistance along parallel paths, R_{path}, is decreased, R_{sh} for the network is reduced, as would be expected in a conventional parallel resistor model. The resistance along a particular conduction path, R_{path}, in the film can be understood with the simple model:

$$R_{path} = R_{SWNT-SWNT} + R_{SWNT} \quad (2)$$

where $R_{SWNT-SWNT}$ and R_{SWNT} are the intertube and intratube SWNT resistances, respectively. Many reports have stated that conductance in SWNT networks is overwhelmingly a function of $R_{SWNT-SWNT}$, due to the large intertube resistance, which has been shown to be orders of magnitude higher than the intratube resistance.[21,22] However, these reports are based on polydispersed SWNT networks, and in the case of primarily homogeneous SWNT films, there are several factors that suggest R_{SWNT} and $R_{SWNT-SWNT}$ are of closer magnitudes. First, these previous reports are based on near ballistic charge transport along carbon nanotubes, with an approximate mean free path, λ, on the order of 1 μm. While these reports present best case resistances, significant variability in the intratube resistance has been shown.[23] Furthermore, in SWNT networks, the mean free path of a charge carrier is significantly reduced, due to the existence of defects on the surface. The density of defects are considerably increased through processes such as acid-based purification and ultrasonication that are employed to achieve highly dispersed, homogeneous solutions of purified nanotubes.[24,25] While λ is not known for these films, it is reasonable to expect it to be substantially lower than values used in previous studies that compared R_{SWNT} to $R_{SWNT-SWNT}$. Also, as shown by Fuhrer *et al.*, the $R_{SWNT-SWNT}$ for nanotubes of similar electronic type is 2 orders of magnitude lower than the $R_{SWNT-SWNT}$ between metallic and semiconducting SWNTs.[26] Therefore, in contrast to past comparisons of R_{SWNT} to $R_{SWNT-SWNT}$, SWNT films of homogeneous electronic behavior may have values for R_{SWNT} and $R_{SWNT-SWNT}$ closer in magnitude, which merits investigation into the impact that both have on the overall conductivity of the film.

$R_{SWNT-SWNT}$ is limited by a tunneling barrier between nanotubes in electrical contact. As the density of charge carriers, n, is increased in the SWNT film, local electric fields are created at SWNT interfaces that can modify the shape and height of tunnel barriers.[12] Futhermore, the hole doping process used in this study has been shown by Barnes *et al.* to increase tunneling probability in monodispersed SWNT films, thereby resulting in lower $R_{SWNT-SWNT}$.[27] A similar observation of reduced intratube resistance after chemical treatment was observed by Nirmalraj *et al.*[28]

The governing electrical conduction of R_{SWNT} can be understood with regard to the general description of conductivity of materials:

$$\sigma = ne\mu \quad (3)$$

where e and μ are the electronic charge and charge mobility, respectively. As a result of the chemical treatment used to dope films in this study, holes were injected into the valence band of SWNT films, yielding p-type nanotubes.[29] As such, n is equal to the density of holes, p, below the intrinsic Fermi energy, E_{Fi}. From eq 3, it is expected that the conductivity of individual SWNTs will be enhanced as either p and/or μ are increased. Thus, since both R_{SWNT} and $R_{SWNT-SWNT}$ can be decreased by the injection of additional p-type charge carriers, hole doping SWNT films can reduce R_{path}, irrespective to which resistance dominates total conduction.

The total density of holes is found by integrating the density of holes per unit energy, $p(E)$, over all energies below E_{Fi}. The value $p(E)$ is equal to the product of the density of states below E_{Fi}, $g_v(E)$, and the hole occupation probability, defined in eq 1. It follows that the total density of holes, p, is

$$p = \int p(E)dE = \int_{-\infty}^{E_{Fi}} g_v(E)[1 - f(E)]dE \quad (4)$$

Examination of Figure 2b,c with respect to eq 4 suggests that the doping process injects more holes into semiconducting nanotubes than in metallic nanotubes,

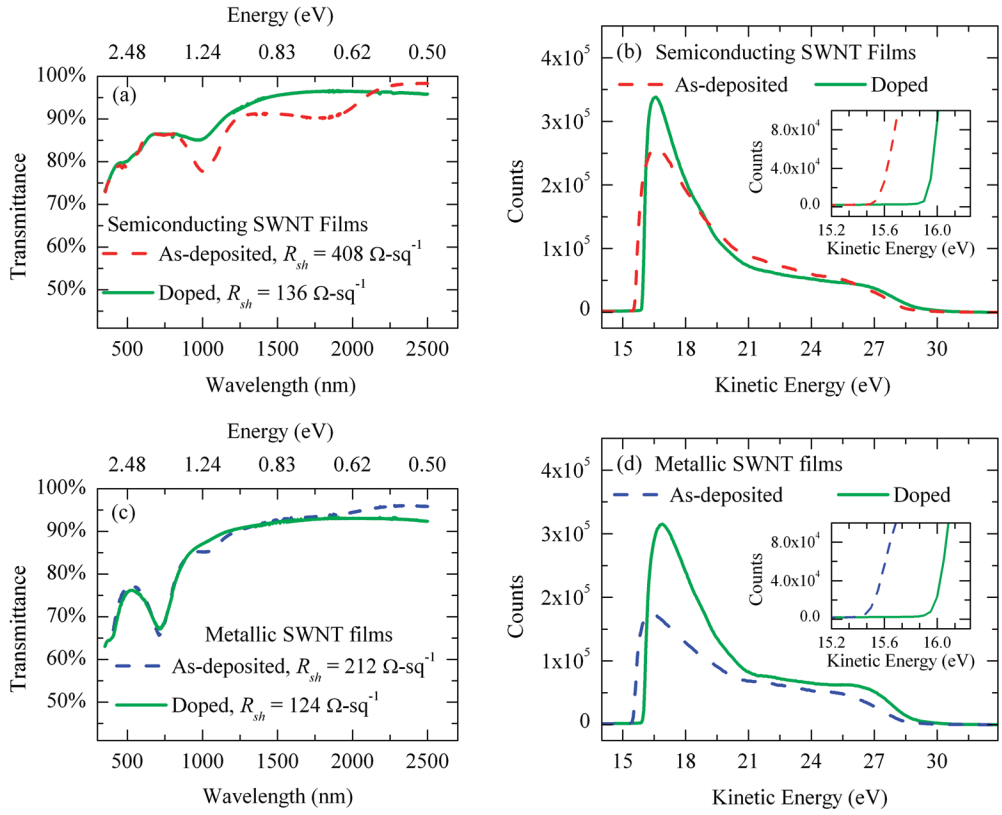

Figure 3. (a) Optical transmittance spectra of as-deposited and doped semiconducting SWNT films. (b) UPS spectra of as-deposited and doped semiconducting SWNT films. (c) Optical transmittance spectra of as-deposited and doped metallic SWNT films. (d) UPS spectra of as-deposited and doped metallic SWNT films.

given the estimated Fermi level position in the energy band structure and the corresponding hole occupation probability.

Impact of Chemical Doping. To confirm the level of hole doping that occurs in as-deposited and doped SWNTs, complementary ultraviolet photoelectron spectroscopy (UPS), electrical sheet resistance, and UV−vis−NIR spectroscopy measurements were carried out on representative monodispersed SWNT films (Figure 3). The UV−vis−NIR spectra of an as-deposited and doped semiconducting SWNT film are shown in Figure 3a. As expected, the sheet resistance is reduced from 408 to 136 $\Omega \cdot sq^{-1}$ after chemical treatment and the S_{11} and S_{22} optical transitions are bleached. In the UPS spectra in Figure 3b, a shift of the low kinetic energy edge can be seen after doping the semiconducting SWNT film, which is indicative of an increase in the surface work function (see Supporting Information).[30] A total surface work function increase of 0.4 eV is observed in doped semiconducting SWNTs, which is similar to the expected Fermi level shift from bleaching of the S_{11} and S_{22} transitions from the transmission spectra in Figure 2. These results are consistent with other reports that show a shift in the Fermi level of SWNTs after doping.[10,29] It must be noted that the surface work function determined by UPS measurements includes the Fermi level position of the sample as well as any surface dipoles created on the surface and is not the ionization potential of the SWNT film. Further discussion is included in the Supporting Information.

Shown in Figure 3c are the UV−vis−NIR spectra of an as-deposited and a doped metallic SWNT film. The optical behavior of the small percentage of semiconducting SWNTs remaining in the metallic film suggests that the initial Fermi level position is in a similar location as the as-deposited semiconducting SWNT film. The surface work function of an as-deposited metallic SWNT film derived from UPS measurements in Figure 3d provides further verification of this observation. After doping *via* chemical treatment, the surface work function is shifted by a similar amount as the semiconducting SWNT film. This corresponds to a small reduction in the absorption intensity of the M_{11} intraband energetic transition derived from doping and a reduction in the electrical sheet resistance from 212 to 124 $\Omega \cdot sq^{-1}$. The change in R_{sh} for the metallic SWNT film is considerably smaller than the change in resistance seen for the semiconducting film after doping. As illustrated in Figure 2c, a Fermi level shift that does not exceed the energy of the first metallic van Hove singularity results in substantially fewer holes, *p*, being injected into metallic SWNTs in comparison to the total number of holes gained by semiconducting SWNTs. These results provide experimental support of the estimated shifts in the Fermi level energy of the SWNT films due to doping, shown in Figures 1b,c and 2b,c. Therefore, the observed

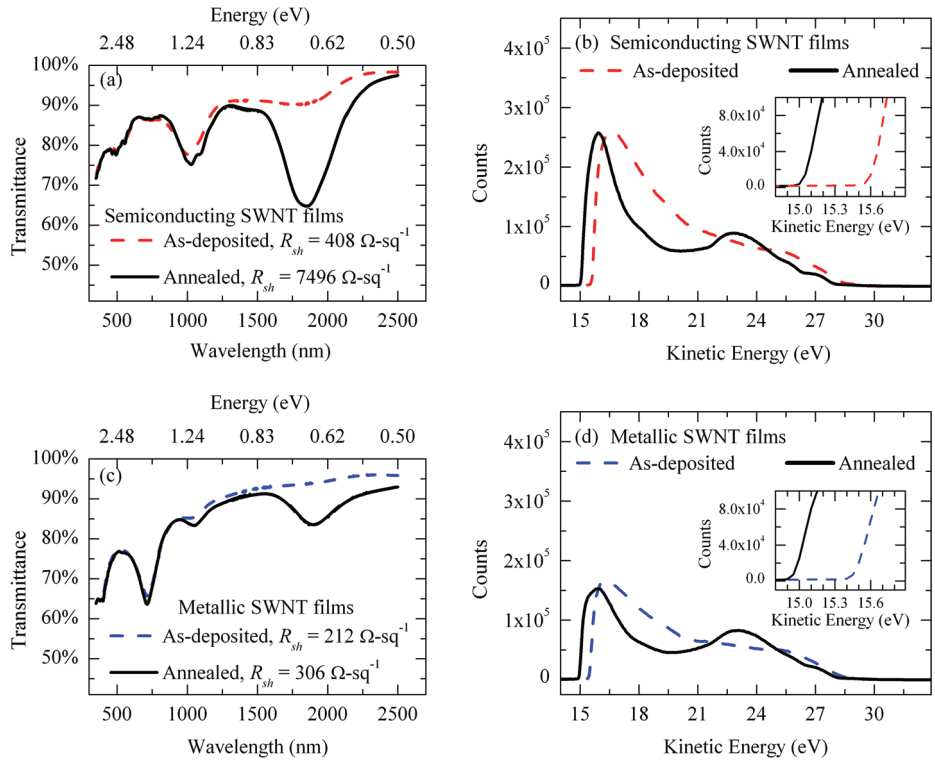

Figure 4. (a) Optical transmittance spectra of as-deposited and annealed semiconducting SWNT films. (b) UPS spectra of as-deposited and annealed semiconducting SWNT films. (c) Optical transmittance spectra of as-deposited and annealed metallic SWNT films. (d) UPS spectra of as-deposited and annealed metallic SWNT films.

smaller sensitivity of R_{sh} of the metallic SWNT film in comparison to the sensitivity of R_{sh} of the semiconducting SWNT film is consistent with the previous discussion of the impact of increased charge carriers on the magnitude of R_{path}. Also, other studies have shown similar trends.[12,19]

Impact of Annealing SWNT Films. In order to determine the optoelectronic impact of oxygen adsorption on the surface of the SWNTs in prepared films, as-deposited SWNT films were annealed at 200 °C and characterized. It has previously been established that oxygen species adsorbed on the surface of SWNTs can act as hole dopants in SWNT films.[12,19] However, the Fermi level shift induced by these dopants has not been verified. Shown in Figure 4a,b are the optical transmittance and UPS spectra of a semiconducting SWNT film as-deposited and after annealing. After annealing, the following is observed: (a) an increase in the S_{11} absorption peak in the film transmittance spectrum, (b) a shift in the surface work function to a lower energy, and (c) an increase in the sheet resistance of the film from 408 to 7496 $\Omega \cdot \mathrm{sq}^{-1}$. As supported by XPS measurements (see Supporting Information), much of the adsorbed oxygen dopants present on the as-deposited SWNT film surface are removed during the annealing process. Therefore, an increase in the S_{11} electronic interband transition will be observed, as electrons replace hole dopants in the valence band up to the first van Hove singularity. Also, the surface work function decrease of approximately 0.5 eV is consistent with a shift of E_F to higher energies due to the loss of hole dopants. Finally, because oxidation from adsorbed oxygen resulted in the degenerate doping of semiconducting SWNTs, R_{sh} is increased by more than an order of magnitude after annealing, as E_F is shifted from within the valence band to a level inside the energy band gap. A similar trend of increased electrical resistance was reported by Wu *et al.*[13]

The optical spectra of an as-deposited and annealed metallic SWNT film are shown in Figure 4c. The sheet resistance increased from 212 to 306 $\Omega \cdot \mathrm{sq}^{-1}$. The metallic SWNT film has a much smaller increase in sheet resistance after annealing than the semiconducting SWNT film, even though a similar change in work function is observed (Figure 4d), along with a similar reduction in adsorbed oxygen (Supporting Information). Unlike semiconducting SWNTs that contain an energy band gap with no density of electronic states above the first van Hove singularity, metallic SWNTs have a nonzero density of states throughout the band structure and therefore remain conductive even after annealing. UPS measurements confirm that the surface work function is similar for both annealed semiconducting and metallic SWNT films with each reaching a value of ~4.1 eV after annealing. The significant work function reduction in both semiconducting and metallic SWNT films after annealing is indicative of the considerable amount of p-type doping in as-deposited SWNT films. Table 1 summarizes the observed surface work functions for the

TABLE 1. Summary of SWNT Film Surface Work Functions Determined from UPS Spectra (R_{sh} in Parentheses)

	metallic film (eV)	semiconducting film (eV)
as-deposited	4.5 (212 $\Omega \cdot sq^{-1}$)	4.6 (408 $\Omega \cdot sq^{-1}$)
doped	5.0 (124 $\Omega \cdot sq^{-1}$)	5.0 (136 $\Omega \cdot sq^{-1}$)
annealed	4.1 (306 $\Omega \cdot sq^{-1}$)	4.1 (7496 $\Omega \cdot sq^{-1}$)

SWNT films analyzed in this study. Also included in the table are the R_{sh} values measured for each case.

CONCLUSIONS

In summary, semiconducting and metallic SWNT films were prepared, and their optoelectronic properties were compared, focusing on the properties that are important for transparent electrode applications in organic electronics. The nanotube film composed of degenerately doped semiconducting SWNTs exhibited lower transmission losses in the optical wavelength range most important to OPVs and OLEDs, in addition to slightly higher electrical conductivity Without specific measurements at the individual nanotube scale, we cannot definitively state that the semiconducting SWNTs are more conductive than metallic SWNTs after chemical treatment. However, we can conclude that a greater number of free charge carriers are injected into doped semiconducting SWNTs than in metallic SWNTs due to the distinct differences in their electronic density of states. Photoelectronic spectroscopy, R_{sh} evaluation, and UV−vis−NIR were presented in this work to provide experimental corroboration of this theoretical conclusion. Free charge carriers injected into SWNTs contribute to nanotube networks with significantly high electrical conductivity due to the decrease in electrical resistance at both the intra- and inter-nanotube scale. While this effect is most likely the dominating factor in conductivity improvement *via* chemical treatment, other authors have also contributed R_{sh} reductions to surfactant removal and film densification.[3]

The results of this report suggest that the 1-D nature of SWNTs requires an unconventional approach to maximize their utility in electronic devices. Not only is the metallic absorption peak at the M_{11} energy transition positioned in a spectral range most important to organic electronics (~700 nm) but also it is not as susceptible to removal as are the S_{11} and S_{22} peaks in semiconducting SWNTs. As a result, SWNT films that contain a large portion of metallic SWNTs will also exhibit similar transmission losses in the visible spectrum as is evident in the doped polydispersed SWNT films presented in other works.[1,2,10,11] Therefore, in contradistinction to traditional methods to achieve high conducting, visibly transparent electrodes that only attempt to utilize metallic constituents, doped semiconducting SWNTs may provide an alternative pathway to achieve highly conductive films. However, as shown in this report, the lower sensitivity of R_{sh} in metallic SWNTs to the Fermi level position and surface work function suggest that the electrical properties of metallic films will be more stable than that seen in semiconducting tubes. This stability may present unique application opportunities for networks of metallic nanotubes. Data shown from our study show that it is possible to create highly conductive metallic nanotube networks over a range of work functions, allowing the creation of a low work function negative electrode in organic electronics. Nonetheless, the separation of CNTs into homogeneous types provides clear advantages to the production of highly conductive transparent CNT electrodes which are difficult to obtain using heterogeneous films.

EXPERIMENTAL SECTION

Transparent SWNT films were prepared on glass substrates using a method similar to that developed by Wu *et al.*[13] Monodispersed SWNT solutions of metallic and semiconducting SWNTs with ≥95% homogeneity by electronic type were purchased from NanoIntegris with a SWNT diameter range of 1.2−1.6 nm. SWNT solutions were diluted and subsequently vacuum filtered through mixed cellulose ester (MCE) membranes with a diameter of 47 mm and a pore size of 100 nm. The MCE membrane was then transferred to the desired substrate (either glass or a gold foil), where the membrane was dissolved in successive acetone baths, leaving behind the SWNT film on the substrate.

Chemical treatment of the SWNT films was performed by immersing the films into solution for 45 min. The films were first immersed into HNO_3, removed, and carefully air blown dry, subsequently heated on a hot plate at 90 °C for 2 min to remove any residual solution on the substrate, and then immersed into thionyl chloride ($SOCl_2$). After removing the film from the $SOCl_2$ bath, the film was blown dry with air and heated on the hot plate for 2 min at 90 °C. The final heating step was proven effective to eliminate optical transmission losses in the visible range by preventing the soft haze that forms on the substrate from $SOCl_2$ exposure. SWNT films exposed to chemical treatment are referenced as "doped" in this report. SWNT films not exposed to chemical treatment are referenced as "as-deposited".

SWNT films were annealed by placing in vacuum at 200 °C overnight.

Sheet resistance (R_{sh}) of the SWNT films was measured using the transmission line method.[31] Silver metal was e-beam deposited on the films through a shadow mask to define fine metal lines on the SWNT films. The spacing between the lines was linearly increased from 0.9 to 6.9 mm. R_{sh} was derived from the slope, m, of the plot of the two-point resistance between adjacent lines *versus* line spacing using

$$m = \frac{R_{sh}}{w} \tag{5}$$

where w is the width of the metal line.

Optical spectra for each SWNT film were measured using a Cary 5E UV−vis−NIR dual-beam spectrophotometer. Because each film was deposited onto glass substrates, a glass reference was used such that the spectra obtained provide an assessment of the transmittance of the SWNT film.

Acknowledgment. We would like to thank the National Science Foundation under the Science and Technology Center

DMR-01209667 (S.G. and N.R.A.), CHE-0836096 (A.M.), and NSF-Chemistry CHE-0517963 (N.R.A.) for financial support.

Supporting Information Available: XPS survey scan and high-resolution oxygen 1 s scan (SI 1), high-resolution C(1s) and Cl(2p) XPS spectra for as-made and doped semiconductor and metallic samples (SI 2), description of ultraviolet photoelectron spectroscopy and determination of surface work function and ionization potential (SI 3), XPS survey scan showing oxygen desorption after annealing semiconductor and metallic SWNT films (SI 4). This material is available free of charge *via* the Internet at http://pubs.acs.org.

REFERENCES AND NOTES

1. Zhang, D.; Ryu, K.; Liu, X.; Polikarpov, E.; Ly, J.; Tompson, M. E.; Zhou, C. Transparent, Conductive, and Flexible Carbon Nanotube Films and Their Application in Organic Light-Emitting Diodes. *Nano Lett.* **2006**, *6*, 1880–1886.
2. Pasquier, A. D.; Unalan, H. E.; Kanwal, A.; Miller, S.; Chhowalla, M. Conducting and Transparent Single-Wall Carbon Nanotube Electrodes for Polymer-Fullerene Solar Cells. *Appl. Phys. Lett.* **2005**, *87*, 203511.
3. Geng, H.-Z.; Ki, K. K.; Kang, P. S.; Young, S. L.; Chang, Y.; Young, H. L. Effect of Acid Treatment on Carbon Nanotube-Based Flexible Transparent Conducting Films. *J. Am. Chem. Soc.* **2007**, *129*, 7758–7759.
4. Gordon, R. G. Criteria for Choosing Transparent Conductors. *MRS Bull.* **2000**, *25*, 52–57.
5. Arnold, M. S.; Suntivich, J.; Stupp, S. I.; Hersam, M. C. Hydrodynamic Characterization of Surfactant Encapsulated Carbon Nanotubes Using an Analytical Ultracentrifuge. *ACS Nano* **2008**, *2*, 2291–2300.
6. Tanaka, T.; Jin, H.; Miyata, Y.; Fujii, S.; Suga, H.; Naitoh, Y.; Minari, T.; Miyadera, T.; Tsukagoshi, K.; Kataura, H. Simple and Scalable Gel-Based Separation of Metallic and Semiconducting Carbon Nanotubes. *Nano Lett.* **2009**, *9*, 1497−1500.
7. Odom, T. W.; Huang, J. L.; Kim, P.; Lieber, C. M. Atomic Structure and Electronic Properties of Single-Walled Carbon Nanotubes. *Nature* **1998**, *391*, 62–64.
8. Mintmire, J. W.; White, C. T. Universal Density of States for Carbon Nanotubes. *Phys. Rev. Lett.* **1998**, *81*, 2506–2509.
9. Itkis, M. E.; Niyogi, S.; Meng, M. E.; Hamon, M. A.; Hu, H.; Haddon, R. C. Spectroscopic Study of the Fermi Level Electronic Structure of Single-Walled Carbon Nanotubes. *Nano Lett.* **2002**, *2*, 155–159.
10. Jackson, R.; Domercq, B.; Jain, R.; Kippelen, B.; Graham, S. Stability of Doped Transparent Carbon Nanotube Electrodes. *Adv. Funct. Mater.* **2008**, *18*, 2548–2554.
11. Parekh, B. B.; Fanchini, G.; Eda, G.; Chhowalla, M. Improved Conductivity of Transparent Single-Wall Carbon Nanotube Thin Films *via* Stable Postdeposition Functionalization. *Appl. Phys. Lett.* **2007**, *90*, 121913.
12. Blackburn, J. L.; Barnes, T. M.; Beard, M. C.; Kim, Y.-H.; Tenent, R. C.; McDonald, T. J.; To, B.; Coutts, T. J.; Heben, M. J. Transparent Conductive Single-Walled Carbon Nanotube Networks with Precisely Tunable Ratios of Semiconducting and Metallic Nanotubes. *ACS Nano* **2008**, *2*, 1266–1274.
13. Wu, Z. C.; Chen, Z. H.; Du, X.; Logan, J. M.; Sippel, J.; Nikolou, M.; Kamaras, K.; Reynolds, J. R.; Tanner, D. B.; Hebard, A. F.; Rinzler, A. G. Transparent, Conductive Carbon Nanotube Films. *Science* **2004**, *305*, 1273–1276.
14. Jackson, R.; Graham, S. Specific Contact Resistance at Metal/Carbon Nanotube Interfaces. *Appl. Phys. Lett.* **2009**, *94*, 012109-3.
15. Maruyama, S. Shigeo Maruyama's Fullerene and Carbon Nanotube Site; http://www.photon.t.u-tokyo.ac.jp/~maruyama/kataura/1D_DOS.html (accessed 2/24/2009).
16. Kataura, H.; Kumazawa, Y.; Maniwa, Y.; Umezu, I.; Suzuki, S.; Ohtsuka, Y.; Achiba, Y. Optical Properties of Single-Wall Carbon Nanotubes. *Synth. Met.* **1999**, *103*, 2555–2558.
17. Collins, P. G.; Bradley, K.; Ishigami, M.; Zettl, A. Extreme Oxygen Sensitivity of Electronic Properties of Carbon Nanotubes. *Science* **2000**, *287*, 1801–1804.
18. Grujicic, M.; Cao, G.; Singh, R. The Effect of Topological Defects and Oxygen Adsorption on the Electronic Transport Properties of Single-Walled Carbon-Nanotubes. *Appl. Surf. Sci.* **2003**, *211*, 166–183.
19. Miyata, Y.; Yanagi, K.; Maniwa, Y.; Kataura, H. Optical Properties of Metallic and Semiconducting Single-Wall Carbon Nanotubes. *Phys. Status Solidi B* **2008**, *245*, 2233–2238.
20. Hu, L.; Hecht, D. S.; Gruner, G. Percolation in Transparent and Conducting Carbon Nanotube Networks. *Nano Lett.* **2004**, *4*, 2513–2517.
21. Behnam, A.; Ural, A. Computational Study of Geometry-Dependent Resistivity Scaling in Single-Walled Carbon Nanotube Films. *Phys. Rev. B* **2007**, *75*, 125432.
22. Hecht, D.; Liangbing, H.; Gruner, G. Conductivity Scaling with Bundle Length and Diameter in Single Walled Carbon Nanotube Networks. *Appl. Phys. Lett.* **2006**, *89*, 133112-1.
23. Ebbesen, T. W.; Lezec, H. J.; Hiura, H.; Bennett, J. W.; Ghaemi, H. F.; Thio, T. Electrical Conductivity of Individual Carbon Nanotubes. *Nature* **1996**, *382*, 54–56.
24. Hu, H.; Zhao, B.; Itkis, M. E.; Haddon, R. C. Nitric Acid Purification of Single-Walled Carbon Nanotubes. *J. Phys. Chem. B* **2003**, *107*, 13838–13842.
25. Lu, K. L.; Lago, R. M.; Chen, Y. K.; Green, M. L. H.; Harris, P. J. F.; Tsang, S. C. Mechanical Damage of Carbon Nanotubes by Ultrasound. *Carbon* **1996**, *34*, 814–816.
26. Durkop, T.; Getty, S. A.; Cobas, E.; Fuhrer, M. S. Extraordinary Mobility in Semiconducting Carbon Nanotubes. *Nano Lett.* **2004**, *4*, 35–39.
27. Barnes, T. M.; Blackburn, J. L.; van de Lagemaat, J.; Coutts, T. J.; Heben, M. J. Reversibility, Dopant Desorption, and Tunneling in the Temperature-Dependent Conductivity of Type-Separated, Conductive Carbon Nanotube Networks. *ACS Nano* **2008**, *2*, 1968–1976.
28. Nirmalraj, P. N.; Lyons, P. E.; De, S.; Coleman, J. N.; Boland, J. J. Electrical Connectivity in Single-Walled Carbon Nanotube Networks. *Nano Lett.* **2009**, *9*, 3890–3895.
29. Dettlaff-Weglikowska, U.; Skakalova, V.; Graupner, R.; Jhang, S. H.; Kim, B. H.; Lee, H. J.; Ley, L.; Park, Y. W.; Berber, S.; Tomanek, D.; Roth, S. Effect of $SOCl_2$ Treatment on Electrical and Mechanical Properties of Single-Wall Carbon Nanotube Networks. *J. Am. Chem. Soc.* **2005**, *127*, 5125–5131.
30. Cahen, D.; Kahn, A. Electron Energetics at Surfaces and Interfaces: Concepts and Experiments. *Adv. Mater.* **2003**, *15*, 271–277.
31. Cohen, S. S. Contact Resistance and Methods for Its Determination. *Thin Solid Films* **1983**, *104*, 361–379.